Renewable and Sustainable Energy Reviews 39 (2014) 898–911

Contents lists available at ScienceDirect

Renewable and Sustainable Energy Reviews

journal homepage: www.elsevier.com/locate/rser

Wind-resource atlas of Venezuela based on on-site anemometry observation

Francisco González-Longatt [a,*], Javier Serrano González [b], Manuel Burgos Payán [b], Jesús Manuel Riquelme Santos [b]

[a] School of Electronic, Electrical and Systems Engineering, W2.63, Loughborough, LE11 3TU, United Kingdom
[b] Department of Electrical Engineering, University of Seville, 41092 Seville, Spain

ARTICLE INFO

Article history:
Received 3 March 2014
Received in revised form
8 July 2014
Accepted 19 July 2014
Available online 9 August 2014

Keywords:
Wind potential
Wind power
Wind-resource assessment
Wind speed

ABSTRACT

This paper presents a wind-resource atlas of Venezuela based on wind observations recorded from on-site meteorological stations. Meteorological datasets of 32 weather stations located over northern Venezuela are used in the development of the maps of three main regions in Venezuela: West, Central and East. Hourly observations of wind speed and direction at each anemometer mast, recorded during the period 2005–2007, have been analysed in order to define the statistical description of the wind resource in the studied area. This processed data along with information on elevation and roughness length is used to model the horizontal and vertical extrapolation of wind data and the estimation of the wind resource. An implementation of *Mass-conservation Wind-Flow Model* in OpenWind software is used to calculate the wind resource at each anemometer mast. A distance-squared interpolation method is proposed as the post-processing procedure and blending technique to create each map upon which a Venezuelan wind atlas is then built. Simulation results include two main wind-resource atlases obtained at 80 m height above ground: (i) a traditional map of mean wind speed for each direction; and (ii) a map of power density. Results show that the best wind-energy resources are located in the northern coastal area of Venezuela.

Contents

* Corresponding author.
E-mail addresses: fglongatt@fglongatt.org (F. González-Longatt), javierserrano@us.es (J. Serrano González), mburgos@us.es (M. Burgos Payán), jsantos@us.es (J.M. Riquelme Santos).

http://dx.doi.org/10.1016/j.rser.2014.07.172
1364-0321/

1. Introduction

The Bolivarian Republic of Venezuela is a country located at the northernmost end of South America, and covers a total area of 916,445 km^2 and has a land area of 882,050 km^2. Shaped roughly like an inverted triangle, the country has a 2800-km coastline, and is bounded to the north by the Caribbean Sea and the Atlantic Ocean, to the east by Guyana, to the south by Brazil, and to the west by Colombia (details are shown in Fig. 1) [1,2]. Venezuela is located within the latitude and longitude of 8°00'N and 66°00'W.

Venezuela has the largest electricity consumption in South America (4018 kWh/year per capita) and its electric power system provides electricity to 95% of the Venezuelan population. The peak demand value varies between 16,500 MW and 18,200 MW depending on seasonal conditions. Electricity consumption rises between 4% and 7% per year, and is expected to increase at the same or higher rate over the next 10 years. Total generation capacity installed is 26,550 MW and the generation mix is 65% hydropower, 32% thermal power plants and 3% distributed energy resources. Although the proven oil reserves in Venezuela are claimed to be one of the largest in the world, more aggressive policies on the use of environment friendly electricity generation have been established in recent years in Venezuela. Several academic projects have been reported to promote *renewable-energy resource* installations in numerous areas of Venezuela [3–5], especially for wind power. Several small-scale and off-grid wind-power projects have been developed and two utility-scale wind farms are presently under development in mainland Venezuela: La Guajira (25 MW) [3], and La Peninsula de Paraguaná (100 MW) [2].

A wind-energy map can stimulate wind-energy projects and promote the exploitation of the wind for various applications, including electricity generation, and water pumping for irrigation. It can also become a tool to help decision-makers seek potential investors in this relatively unexploited field. In many countries, government agencies provide wind maps and wind-resource data, but there remain a number of countries where this kind of study has yet to be performed. In this case, independent researchers have conducted such studies and the results have been presented in several scientific papers: Alamdari et al. [6] presented a wind map of Iran based on observed wind-speed data and geographical interpolation, İlkiliç [7] conducted a similar study in Turkey, Đurišić and Mikulović [8] analysed the South Banat region in Serbia, Ahmed analysed the wind resource in South Egypt [9], and Jervase and Al-Lawati [10] presented a similar study for the Sultanate of Oman.

A large-scale wind-power assessment using reanalysis of wind data in the Caribbean region is presented by Chadee and Clarke [11]; this analysis is valid for a global energy assessment, but the level of detail renders it unsuitable for local assessment in Venezuela. There is a wind-speed map of Venezuela currently in existence, which has been publicly available since the 1960s, but there is no information about the data source, quality and relevant information to make this map useful. Other wind maps have been developed in last decade using reanalysis [5], and satellite data [12], and more recently the Venezuelan Government has contracted LNEG – *Laboratório Nacional de Energia e Geologia* [13] to develop a full wind-energy assessment and wind map, but it remains incomplete at the time of writing this paper. Finally, a wind-resource map of Venezuela using on-site hourly-observation anemometry is not currently available and this paper fulfils this lack of information.

This paper is organized as follows: Section 2 briefly describes the analysis method for a wind-resource map; Section 3 presents the input data used to perform the presented study; while Section 4 presents the results obtained and a discussion of their significance. Finally, in Section 5, the conclusions of the performed analysis are provided.

2. Analysis method

A regional assessment of wind and energy resources over a large area must predict the mean wind behaviour in terms of *wind speed* and *direction* and total *annual energy production* (extractable wind energy) for a specific wind turbine at a particular site. Wind-resource

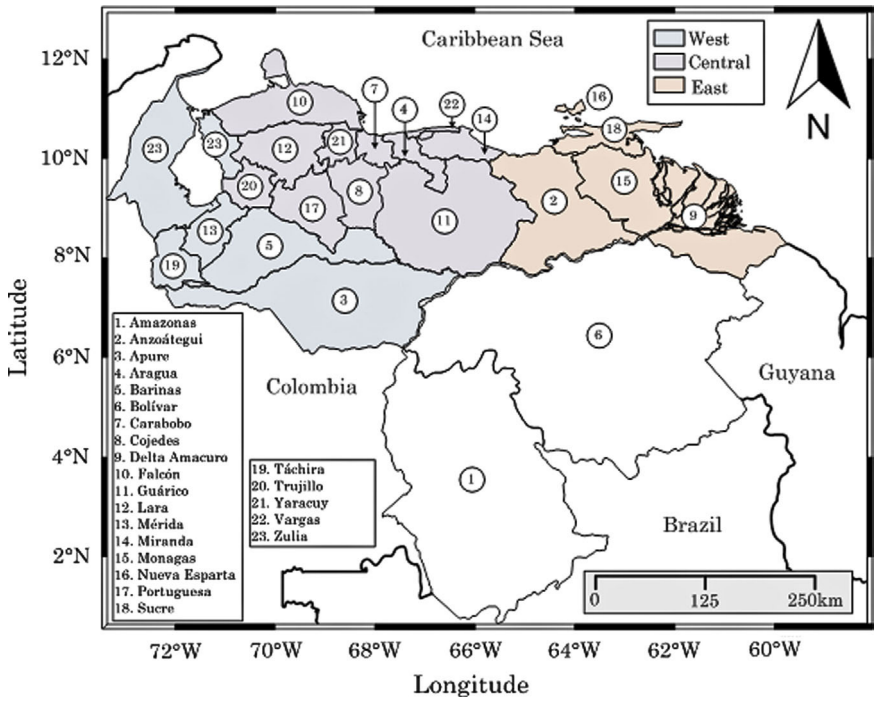

Fig. 1. Geographical location of Venezuela and Political Division.

mapping consists of building a model of the surface of the country or region plus adjacent areas. For each cell, data describing both *terrain elevation* and local *surface roughness* are used for the model. Several methods have been applied to a comprehensive set of the model for the horizontal and vertical extrapolation of wind data as well as for the estimation of wind climate and wind resources. There are several spatial modelling approaches, which can be conveniently classified into four general categories [14]: *conceptual, experimental, statistical*, and *numerical*. This paper uses the *Mass-conservation Wind-Flow Model* to estimate wind resource. This typically entails extrapolating the wind resource measured at one or more meteorological towers to different heights (vertical extrapolation) and over the terrain under study (horizontal extrapolation) by using a *numerical wind-flow model*.

Fig. 2 shows a simplified diagram of the methodology used in this paper in order to create the wind-resource atlas of Venezuela

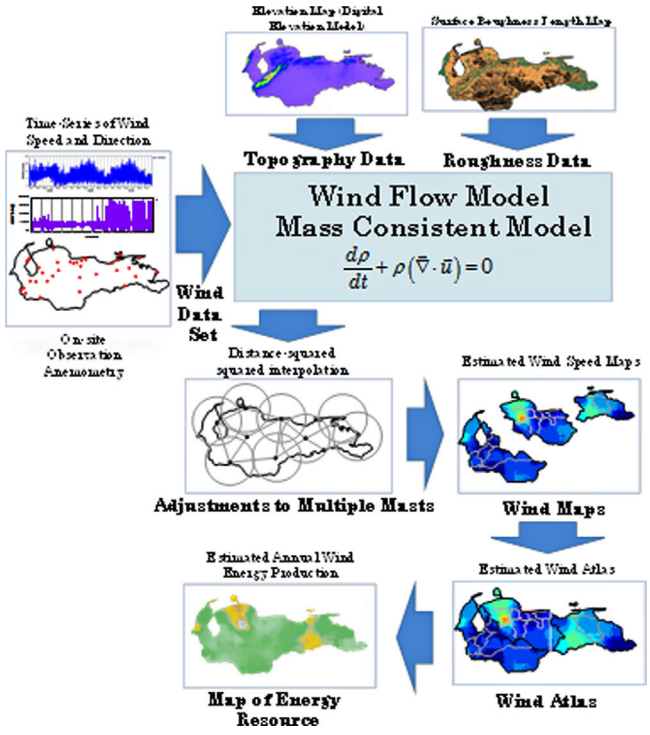

Fig. 2. Methodology used to create Venezuelan wind-energy map: wind-flow modelling using the mass-consistent model.

based on using on-site anemometry observations. The inputs of the wind-flow model essentially consist of (a) *topography data* or an elevation map, (b) *roughness length*, and (c) *statistical description of the wind data measured* at each meteorological station. All this data is used by the wind-flow model in order to create the wind map: wind speed and frequency for each wind direction over the studied surface.

In this paper, the wind resource in the surrounding area of each anemometer mast is evaluated separately. The overall wind-resource map is then computed through merging the results obtained by taking into account each individual mast. Once the wind atlas is created, it is possible to calculate the suitability for wind-power utilization at each location by analysing the wind-power density or the wind-power production (if the wind-turbine model is already known). The main characteristics of each of the above-mentioned calculation modules are described in the following sections.

The principal horizontal extrapolation methods include: (i) Linear Jackson–Hunt wind-flow model, which is a fast, linearized, steady-state *Navier–Stoke* (NS) solver; (ii) *Computational Fluids Dynamics* (CFD) Models, most of which use *Reynolds-averaged NS* (RANS) solvers; and (iii) N*umerical weather prediction* (NWP) models where a full-time, varying 3D physical model of the atmosphere is included (e.g. WRF, MASS, KAMM, and ARPS). Currently, there are several commercial programmes that provide regional wind-resource assessment [15]: WAsP, Meteodyn, AWS Truepower, WinSim, Wind Pro, SiteWind, ARPS, and OpenWind.

2.1. Wind-flow model

Numerous *flow models* (different types and complexities) have been applied for wind-resource assessment purposes. In Fig. 3, a brief overview is given showing the names of certain models and presenting the main classification of the models in terms of their main properties [16]. The typical magnitude of the spatial resolution is given as additional information.

The most popular methods of spatial modelling rely mainly on *numerical* wind-flow models. There are numerous numerical wind-flow models in use by the wind industry today, which are based on a variety of theoretical approaches. All models attempt to solve at least some of the physical equations governing motions of the atmosphere, with varying degrees of complexity. The models fall into four general categories: mass-consistent, Jackson–Hunt, *computational fluid dynamics* (CFD), and *meso-scale numerical weather prediction (NWP)* models.

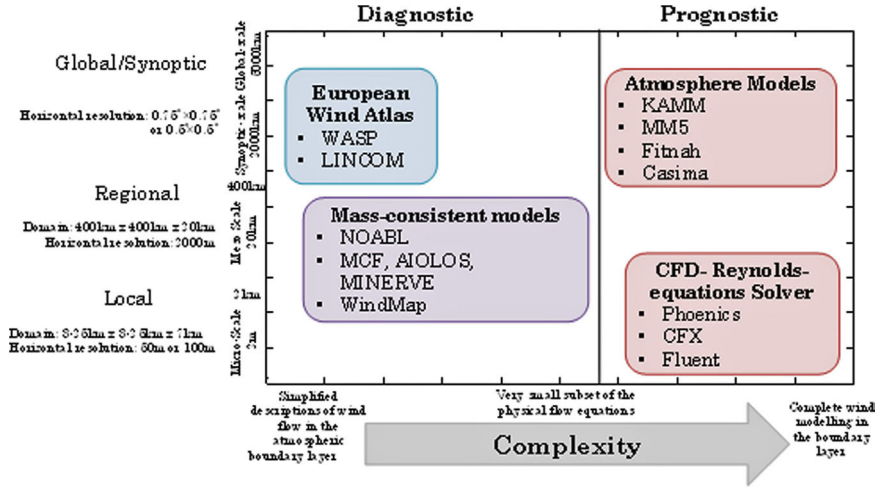

Fig. 3. Overview of flow models applied for wind-energy purposes.

The first generation of numerical wind-flow models developed in the 1970s and 1980s (e.g. NOABL [17] and MINERVE [18]) produced the *mass-consistent models*. The basis all of these models is the *NOABL model* [17], and several modifications or commercial variants, such as MCF, AIOLOS, and WindMap exist. The *mass-consistent models* solve just one of the physical equations of motion: that governing mass conservation [19]. The usual resolution of these models is medium to high and the computational requirement is relatively low when compared with CFD models. This mass-consistent model contains no dynamic equations. It solves the conservation of mass equation to generate 3-D, terrain-dependent, divergence-free wind flow.

In order to perform the wind-resource analysis, in this work the software package OpenWind [20] has been used. This software is an open source platform that enables the calculation of the wind behaviour in the area under study. This package uses a mass-consistent model version based on NOABL code, proposed initially by Phillips in 1979 [17], which made it possible to model height displacements. The wind-flow model currently used by OpenWind is Michael Brower's [19] adaptation, which takes into account the internal boundary layer growth due to the sharp transition in surface roughness [19].

The model strives to conserve momentum while minimizing divergence. It takes account of terrain, roughness, and atmospheric stability. As previously stated, the essential input data to compute this calculation is composed of the wind-behaviour datasets observed in one or more meteorological stations, the elevation map, and the roughness map of the area under study. Once this data is known, it is possible to calculate a wind-resource grid for the studied terrain. The main output data provided by OpenWind is composed of the following values at every point of the discretized terrain: mean wind speed for each wind direction that makes up the wind rose, overall mean wind speed, and inflow angles for each wind direction.

2.2. Adjustments to multiple anemometer masts

Most numerical wind-flow models and software packages, such as WAsP and OpenWind, are designed to use data from just one anemometer mast at a time. These days, however, wind projects usually employ several masts [14]. This poses the practical challenge of combining the information from the various masts in estimating the energy production. One common approach is to divide the project area into sections, to each of which is assigned one mast. The sections may be defined by distance (i.e. the closest mast is assumed to "dominate" the area), or they may be defined by some other criterion, such as topographic similarity (e.g. ridge-top sections are assigned to ridge-top masts) [14].

Another approach involves blending the results obtained by taking into account each meteorological mast. The simulation for each mast is performed separately from the others, and the wind resource for any point within a section is extrapolated from whichever mast to which that section is assigned. A relatively simple blending technique includes weighting the prediction of each mast in accordance with the inverse of the squared distance to each mast. Therefore, in this paper the *distance-squared interpolation* [21,22] is the proposed methodology. This distance-squared interpolation is described by the following equation:

$$\overline{u}(i,j)=\frac{\sum_{k=1}^{N_m} w_k(i,j)u_k(i,j)}{\sum_{k=1}^{N_m} w_k(i,j)} \tag{1}$$

where $\bar{u}(i,j)$ is the interpolated wind speed at the node (i,j), $u_k(i,j)$ is the wind speed at the node (i,j) obtained by the simulation software through taking into account the meteorological station k, and finally, w represents the weights calculated as follows:

$$w_k(i,j)=\frac{1}{d^2} \quad if \quad d\le d_{max}$$
$$w_k(i,j)=0 \quad if \quad d>d_{max} \tag{2}$$

where

$$d=\sqrt{(x_{ij}-x_k)^2+(y_{ij}-y_k)^2}$$

and (x_{ij},y_{ij}), (x_k,y_k) are the geographical coordinates of the node under study and of the k-th meteorological mast, respectively.

2.3. Wind-power density calculation

The wind power (p) available in a certain area, A, crossed by the airflow with a speed (u) can be calculated as the aerodynamic power contained in the airflow (p_w) divided by the area

$$p(v)=\frac{P_w}{A}=\frac{\frac{1}{2}A\rho u^3}{A}=\frac{1}{2}\rho u^3 \tag{3}$$

However, as a consequence of the cubic dependence of power with wind velocity, the mean speed remains an unsuitable measure when assessing the available density power.

It is well known that the statistical behaviour of the wind can be approximated by the *Weibull distribution function* [23], which describes probability, $P(v)$, for a certain wind speed, v, depending on the scale parameter, C, and the shape parameter, K

$$P(u)=\frac{K}{C}\left(\frac{u}{C}\right)^{K-1}\exp\left(-\left(\frac{u}{C}\right)^{K}\right) \tag{4}$$

Scale and shape parameters and mean wind speed are related by means of the following expression:

$$\overline{U}=C\Gamma\left(1+\frac{1}{K}\right) \tag{5}$$

where $\bar{U}$ is the mean wind speed and Γ is the *gamma function*. According to Eq. (5), it is possible to calculate the scale parameter from the mean wind speed in those cases when the shape parameter is known. Finally, the mean *wind-power density*, WPD, can be evaluated as

$$\mathrm{WPD}=\int_{u=0}^{\infty}\frac{1}{2}\rho u^3 P(u)du \tag{6}$$

3. Data sources and preparations

In this section, the data employed to create the wind-resource atlas of Venezuela is presented. This data consists of three subsets used as inputs to the calculation model described in Section 2 (Fig. 2): statistical description of the wind data measured, topography data or elevation map, and roughness length.

3.1. Observed meteorological data and study area

The *Meteorology Service of the Venezuelan Air Force* (MSVAF) has a network of weather stations located at both rural and urban sites, mainly in airports and military bases, in order to collect and process data for the purpose of producing forecasts of weather conditions. The MSVAF meteorological network consists of 37 weather stations deployed across Venezuelan territory (Fig. 4). Despite the fact that wind speeds and directions are measured and recorded in many locations across Venezuela, the wind resources have yet to be completely evaluated.

The Bolivar state and Amazonas state have been excluded from this study owing to the scarcity of meteorological stations in these

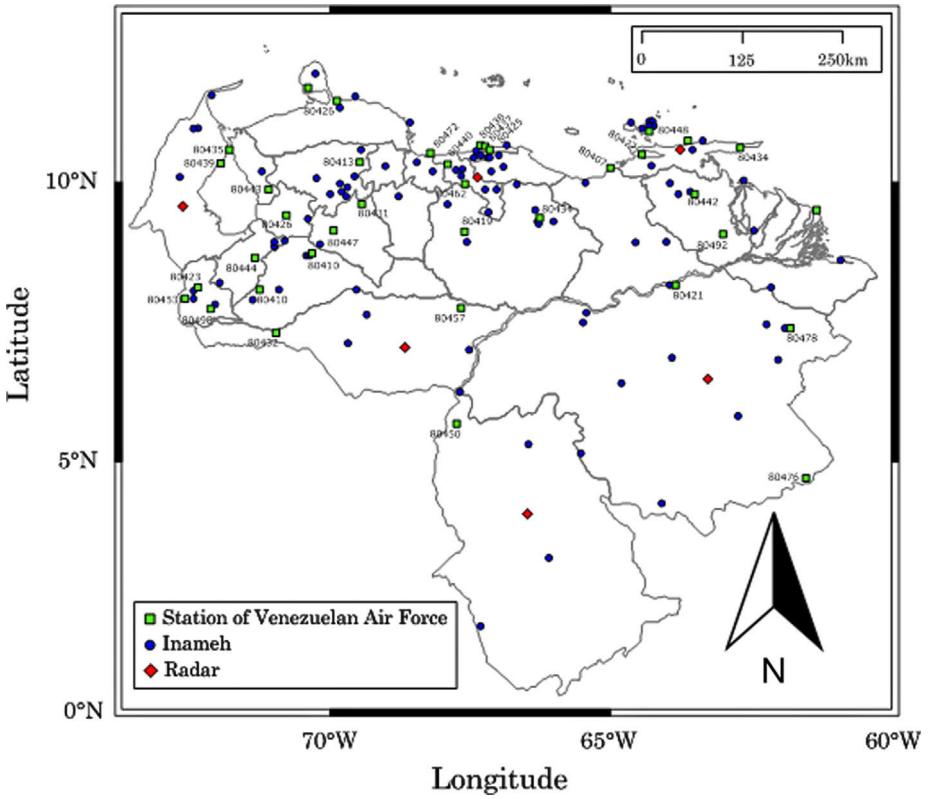

Fig. 4. Geographical location of the weather station network in Venezuelan territory.

regions for the performance of a wind-resource assessment with sufficient accuracy. It is worth noting that these two regions are the most extensive in surface area and correspond to 45.38% of the overall surface of Venezuela. Nevertheless, due to the dense vegetation and forest they constitute the least populated areas (approximately 6% of the total population of Venezuela).

In this study, the data collected at 32 weather stations has been used. It should be borne in mind that five of the anemometer masts available have been excluded: in three of these masts, the available time period of registration was insufficient to perform an accurate analysis of the wind behaviour, and the other two masts were located outside the area covered in this study.

Table 1 shows the main features of each weather station considered: geographical location, elevation above sea level, register period, mean speed, and mean wind-power density. The collection of the data was performed between the years 2005 and 2007 by means of an hourly recording of the wind speed and incoming wind direction at a height of 10 m.

The study area consists of 55.62% of the overall surface of Venezuelan territory and includes 23 states. The surface under study has been divided into three regions in order to better clarify the results obtained:

- *West region:* Barinas, Mérida, Trujillo Táchira, Zulia, and Apure.
- *Central region:* Guárico, Aragua, Carabobo, Distrito Capital, Miranda, Vargas, Cojedes, Falcón, Lara, Portuguesa, and Yaracuy.
- *East region:* Anzoátegui, Delta Amacuro, Monagas, Nueva Esparta, and Sucre.

The main features of these regions in terms of geographical limits, population, and surface area can be observed in Table 2, and the geographical location is shown in Fig. 1.

3.2. Statistical description of the wind data

The wind-resource data has been validated and then analysed to generate the main statistics indicator in order to characterize the local wind resource at each weather station.

On-site anemometry data has been used to characterize the observed wind resource. Figs. 5–7 show the geographical location of each of the considered meteorological stations based on the three regions under consideration. The percentage of wind-power density corresponding to each wind direction is presented in the form of a 12-direction-sector wind rose at a meteorological mast. It should be borne in mind that the amount represented for each wind direction is the percentage calculated by taking into account the total density power corresponding to each of the meteorological stations (see last column of Table 1).

Results show the best wind-energy resources are located in the northern coastal area of Venezuela.

3.3. Topography data

The air flow and amount of power available from the wind are strongly influenced by the local terrain characteristics. Therefore, a good knowledge of the terrain and its effect on the wind are important for numerical wind-flow modelling purposes. The wind-speed profile is affected by topographic features, such as escarpments, hills, and ridges. A change in topography causes an immediate response by the boundary layer, thereby producing the acceleration of flow over the crest of the hill; this is approximately twice the original surface wind speed. This phenomenon, which is known as the *speed-up factor* [24], is associated with deceleration of the wind and turbulence on the leeward side. Accurate, high resolution topographic data is essential for any numerical wind-flow modelling. In this paper, a spatial resolution of 1000 m is used

Table 1
Description and geographical coordinates of weather stations in Venezuela.

ID code	Station name	Geographical coordinates		State ID	Elevation (m above sea level)	Register period	Mean speed (m/s)	Mean density power (W/m^2)
		Latitude (deg.)	Longitude (deg.)					
80435	Acarigua	9.55	−69.23	17	226	2005–2007	2.36	16.20
80419	Barcelona	10.45	−64.68	2	7	2005–2006	2.52	12.75
80440	Barinas	8.62	−70.22	5	204	2005–2007	2.14	7.46
80410	Barquisimeto	10.23	−69.32	12	613	2005–2007	3.76	42.78
80442	Calabozo	8.93	−67.42	11	101	2005–2007	2.31	11.56
80432	Carrizal	9.42	−60.92	14	835	2005	2.13	11.94
80492	Ciudad Bolívar	8.15	−63.55	6	160	2005–2007	3.24	28.48
80403	Colon	8.03	−72.25	19	43	2007	1.94	11.20
80420	Coro	11.42	−69.68	10	1435	2005–2007	5.18	107.47
80437	Cumana	10.45	−64.12	180	16	2007	4.71	110.14
80428	El Vigía	8.63	−71.65	23	2	2005–2007	1.33	3.22
80448	Guanare	9.08	−69.73	17	103	2005–2007	1.67	7.01
80423	Guasdualito	7.23	−70.80	3	163	2005–2007	1.38	2.61
80476	Guiria	10.58	−62.30	18	130	2006	2.56	39.79
80439	La Cañada	10.52	−71.65	10	13	2006–2007	2.98	21.74
80407	Maiquetía	10.60	−66.98	22	63	2005–2007	1.22	12.36
80413	Maracaibo	10.23	−71.73	23	65	2005–2007	2.66	24.49
80435	Maracay	10.25	−67.65	4	436	2005–2007	1.94	5.83
80425	Maturín	9.75	−63.18	2	68	2006–2007	2.96	21.68
80438	Mene Grande	9.78	−70.93	23	27	2005–2007	1.28	2.49
80748	Mérida	8.60	−71.18	13	1479	2005–2007	2.53	11.76
80421	Palmichal	10.30	−68.23	9	1000	2005–2007	1.40	4.22
80447	Porlamar	10.92	−63.97	18	24	2005–2007	5.19	110.39
80450	Tumeremo	7.30	−61.45	15	180	2006	1.26	2.71
80431	San Antonio del Táchira	7.85	−72.45	19	377	2005–2007	2.83	46.02
80443	San Fernando	7.68	−67.42	3	47	2006–2007	2.14	9.87
80462	San Juan	9.92	−67.33	11	429	2005–2007	1.28	2.03
80478	San Tomé	4.60	−61.12	2	262	2006	4.10	50.25
80453	Santo Domingo	7.58	−72.07	13	328	2005–2007	1.34	2.43
80472	Valencia	10.17	−67.93	7	582	2005–2007	1.20	3.71
80426	Valera	9.35	−70.62	20	430	2005–2007	1.63	3.38
80434	Valle de la Pascua	9.22	−66.02	11	125	2005–2007	2.90	20.72

Table 2
Main features of analysed zones.

Region	Easternmost longitude (deg.)	Westernmost longitude (deg.)	Northernmost latitude (deg.)	Southernmost latitude (deg.)	Population (Millions)	Surface (km^2)
West	−66.387	−73.351	11.850	6.060	7.4	189,183
Central	−64.754	−70.864	12.197	7.603	16.1	180,091
East	−59.806	−65.722	11.180	7.660	4.2	128,156

for modelling purposes in the topography map. Terrain heights for the meso-scale simulations are derived from the GTOPO30 global data base (USGS EROS Data Centre), which has a horizontal resolution of 30 arcsec.

Fig. 8 shows the elevation map of the northern region of Venezuela. As can be observed, the coastal plain lies at an elevation of less than 200 m. The interior states of Apure, Barinas, and Guárico are between 100 and 500 m altitude, Merida is between 1000 and 1500 m and the highest mountains are located in Los Andes ($>$ 4000 m).

3.4. Surface data

Friction and the pressure gradient are the only significant forces at the lower levels of the atmospheric boundary layer. The *surface roughness* of the ground is the most significant parameter and affects both the velocity profile and the angle of incidence of wind at ground level. In the atmospheric boundary layer, the airflow is slowed down by friction with the surface. As shown in Table 3, this friction depends on the characteristics of the terrain: surface areas with high roughness length (i.e. forests or big cities) slow down the wind, while on the other hand, smoother surfaces (such as water or flat grassy plains) offer less friction and hence the reduction in the wind speed is lower. Therefore, the roughness length has to be taken into account when performing either the horizontal extrapolation or the vertical extrapolation.

In this paper, the roughness length data has been adapted from the data provided by the study performed by NASA in the Amazon Basin [25]. That study calculated the roughness length based on the analysis of several satellite images combined with an algorithm based on the integration of ground measurements of vegetation structure [26]. The physical roughness of the terrain is estimated by an algorithm of a multivariate-regression model developed from filed-measured vegetation structure and remote sensing data. The vegetation structure is translated into roughness by means of theoretical models. Finally, the results are adjusted by taking into account tower measurements of wind speed and the hydrological and meteorological effects [27]. Fig. 9 presents the data provided by the study performed by NASA in the Amazon Basin. The resolution of the data is 1 km and the values of roughness length have been classified in accordance with the criteria shown in Table 3.

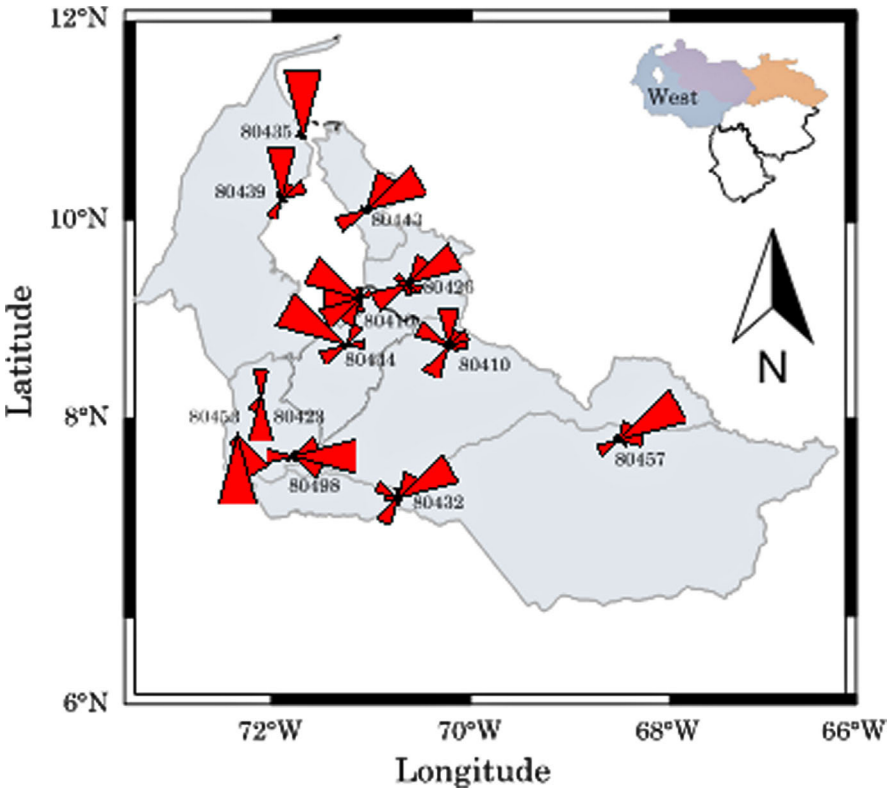

Fig. 5. Characteristics of local wind resources at weather stations in the West region.

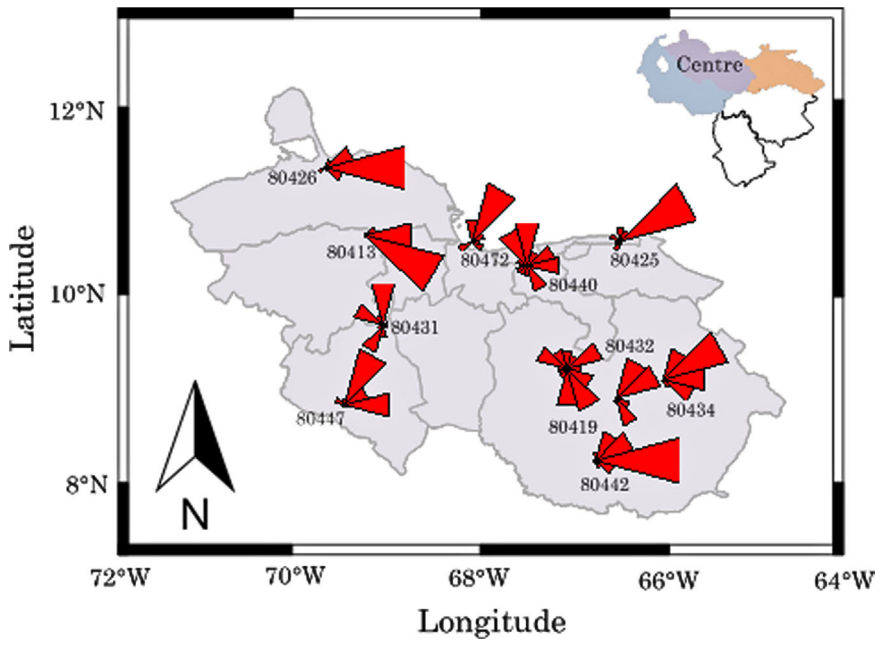

Fig. 6. Characteristics of local wind resources at weather stations in the Central region.

4. Results and discussion

This section presents the results of the wind-resource atlas in the northern regions of Venezuela using the methodology described in Section 2 and the input data presented in Section 3. The Venezuelan wind atlas consists of the three resource maps created using regions defined in Section 3.1. In this paper, wind-flow models are built using horizontal cells of 1 km resolution. In order to simulate the wind behaviour, a *wind-resource grid* has been calculated for each meteorological station available. For computational reasons, the resource grid has a limited size since it is calculated with a resolution of 1 km and a maximum distance (d_{max}) of 150 km from the meteorological station under consideration.

The simulations have been carried out using a PC, Intel i7 920 CPU, 8GB DDR2 running on Microsoft™ Windows® 7 OS. The running time spent on each simulation (one simulation for each meteorological mast) is approximately 3600 s.

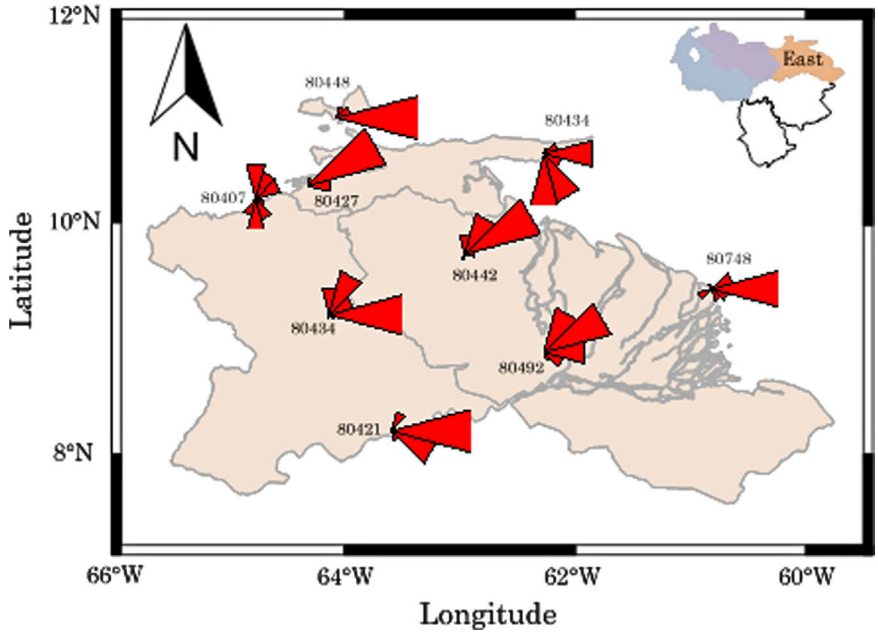

Fig. 7. Characteristics of local wind resources at weather stations in the East region.

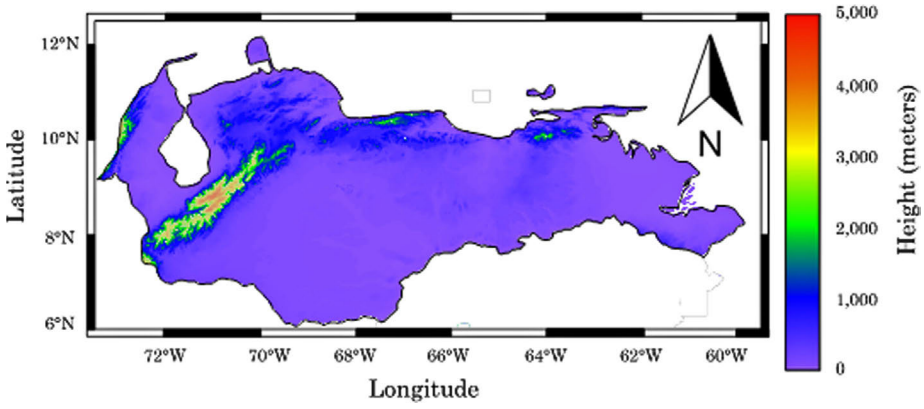

Fig. 8. Elevation map of the northern regions of Venezuela.

Table 3
Typical surface roughness lengths.

Type of terrain	Roughness length, z_0 (m)
Water surface, flat grassy plain	< 0.1
Low crops, occasional large obstacles	0.10–0.25
Bushes, numerous obstacles	0.25–0.50
Regular large obstacle coverage	0.50–1.50
Big cities, intense forest	> 1.50

After all resource grids corresponding to each available meteorological station have been obtained, the grids are then merged using distance-squared interpolation [21,22] to create a wind-resource map.

Two main wind-resource atlases are created as standard outputs in this paper: (i) traditional maps of mean wind speeds; and (ii) maps of power density. The maps are created using the on-site anemometry data. Power-density maps are created by calculating the power of the wind per square metre rotor area for each hour of the year and then by averaging these on a monthly and annual basis. The reason why this latter concept of power density is generally more useful for wind developers than the mean wind speed is that the power of the wind varies with the third power of the instantaneous wind speed. This means that not only does the exploitable wind resource depend on the mean wind speed, but that it also depends on the local wind-speed frequency distribution.

4.1. Wind-speed map

The mean wind speed calculated at a height of 80 m is used to create traditional maps of mean wind speeds for the three regions under consideration. Figs. 10, 11 and 12, show the mean wind speeds for the West, Central and East regions, respectively. It can be observed that the mean wind speed at 80 m ranges between approximately 2 and 13 m/s in each region. Mean wind speeds above 6.0 m/s are found in three regions, especially in the states of Zulia, Falcon, Lara, Anzoátegui, Sucre, and Nueva Esparta.

4.2. Prevailing wind direction map

Figs. 13, 14 and 15 show the prevailing wind direction over the surface of the three zones analysed: West, Centre and East, respectively. The prevailing wind direction is based on hourly on-site observation and provides the direction with the highest percentage of frequency. Results demonstrate that the direction east is the predominant wind direction in northern Venezuela (especially in the East and Central region). This is a consequence of

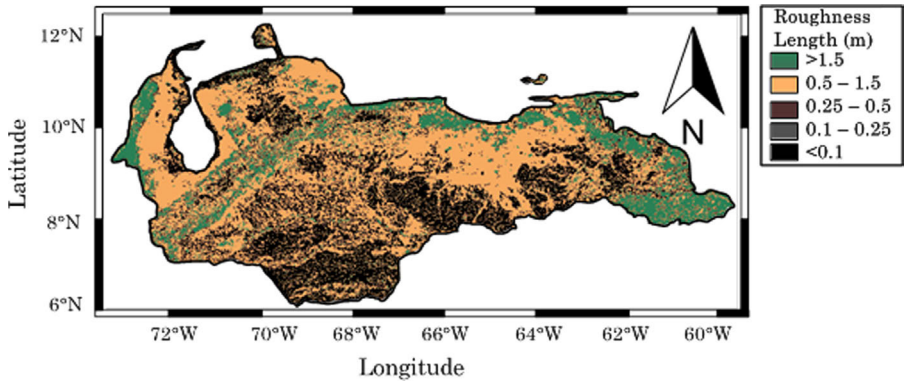

Fig. 9. Roughness length (m) in the northern region of Venezuela.

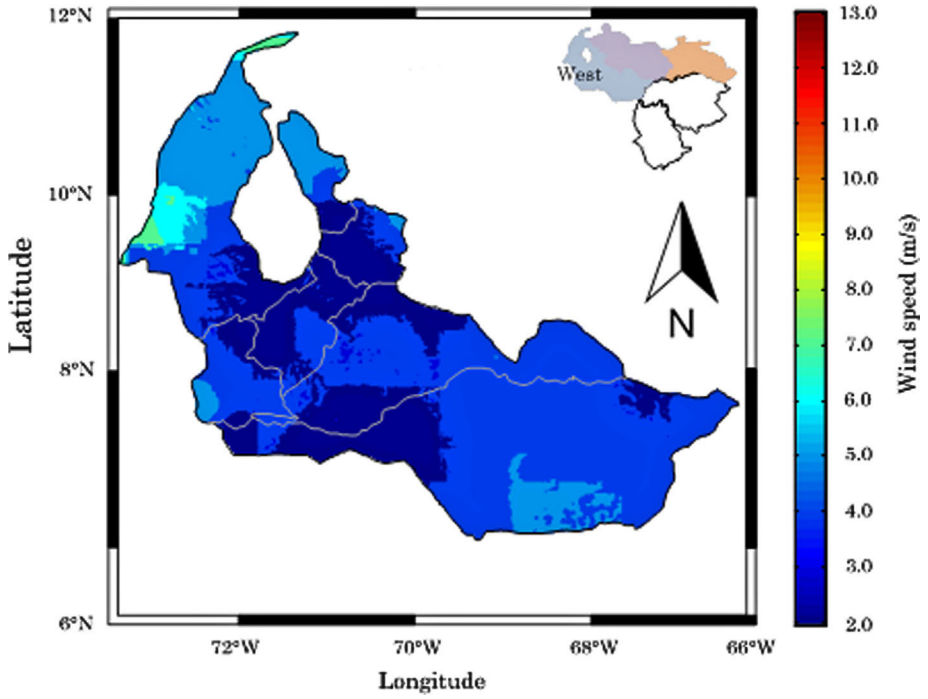

Fig. 10. Map of mean wind speed in West zone at 80 m height.

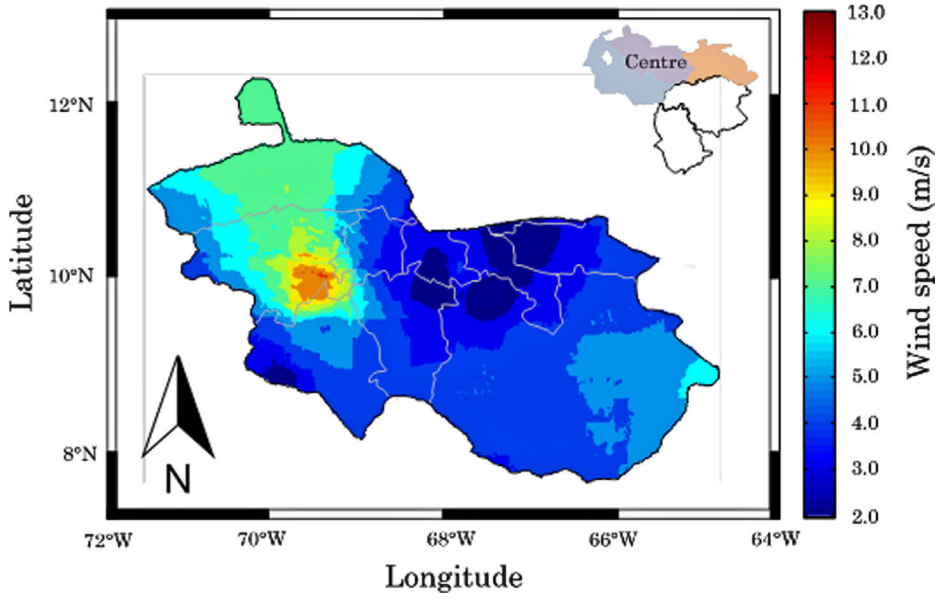

Fig. 11. Map of mean wind speed in Central zone at 80 m height.

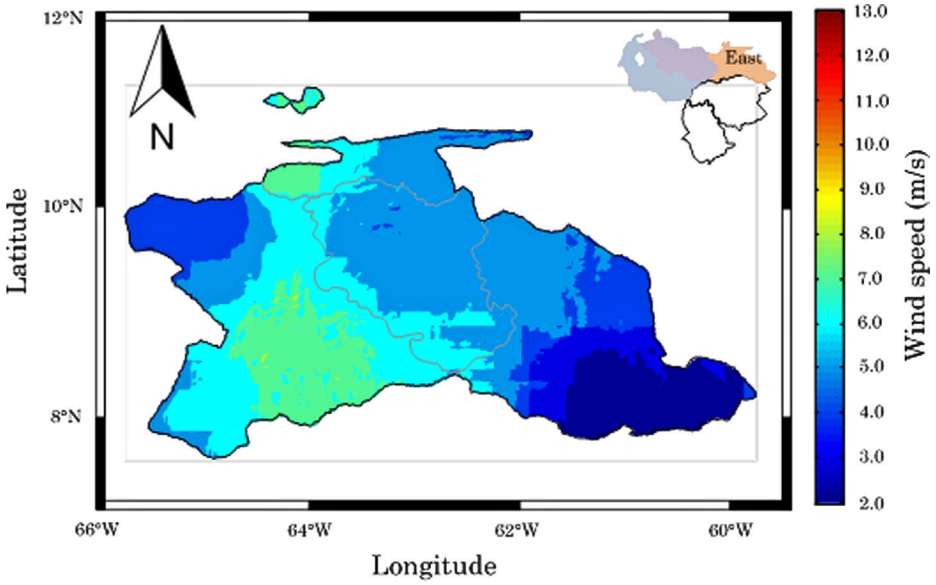

Fig. 12. Map of mean wind speed in East zone at 80 m height.

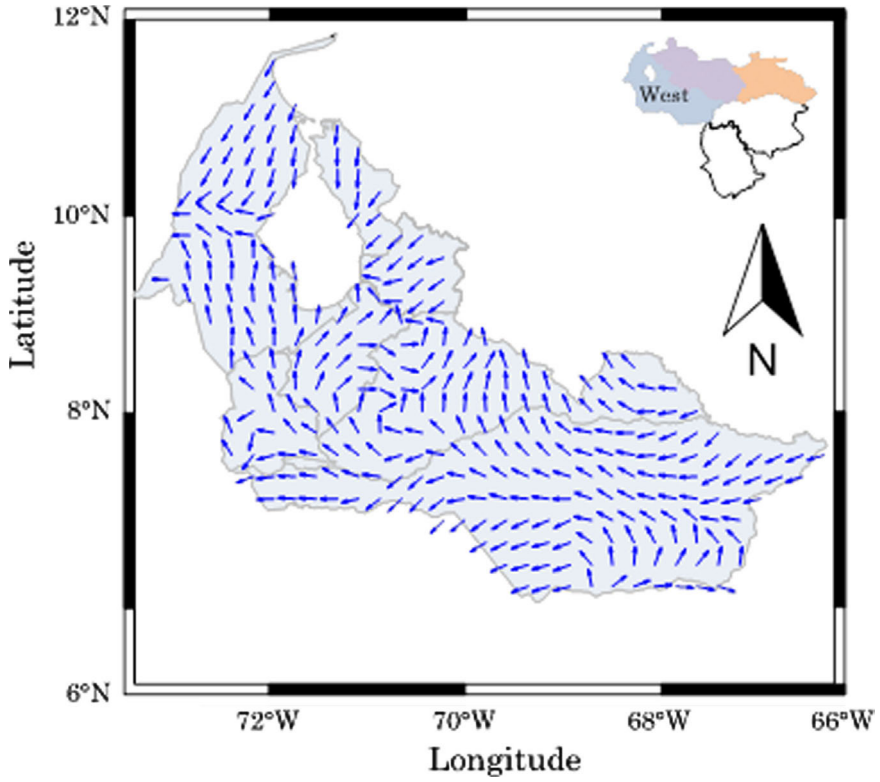

Fig. 13. Map of prevailing wind direction in the West region at 80 m height.

the influence of the Atlantic Northeast trade winds. The wind in northern Venezuela is relatively stable and wind direction is mostly constant all year round, mainly due to the tropical climate with similar temperatures all year round.

The topography of Venezuela has impact on the prevailing wind direction; this is especially true in the West region where the direction east is still dominant, but there are significant local changes caused by the presence of the Andes Mountains at the westernmost part of Venezuela, where a maximum altitude of 4978 m is reached in the Pico Bolivar.

4.3. Wind-power density map

The methodology described in Section 2 has been used to calculate wind-power density at a height of 80 m for each of the regions under consideration. Figs. 16, 17 and 18 show the wind-power density map (W/m^2) for the three regions: West, Central and East, respectively. Wind-power densities from 50 W/m^2 up to 600 W/m^2 are available in the area of Venezuela studied. The best wind conditions are found in the central zone, especially the states of Lara (where the wind-power density achieves values higher

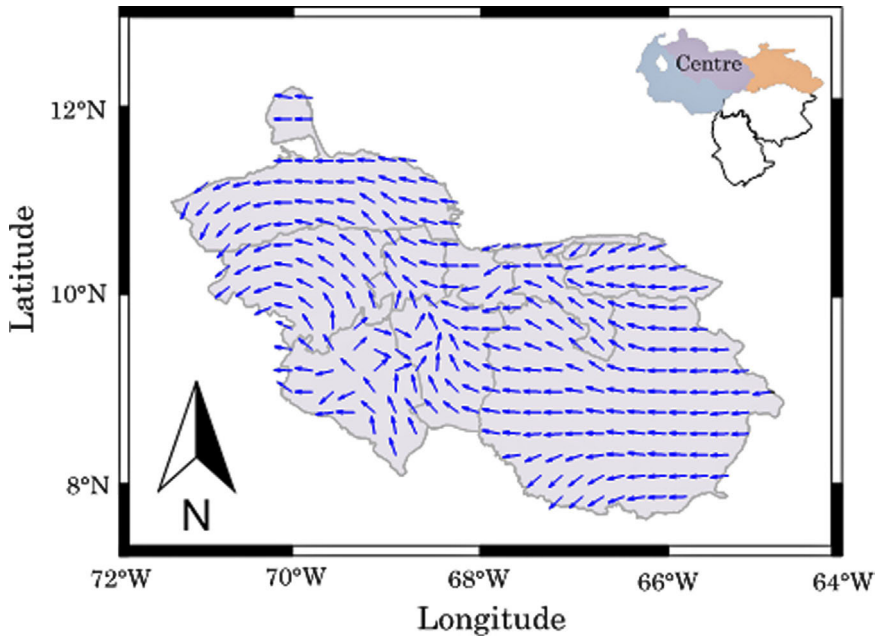

Fig. 14. Map of prevailing wind direction in Central region at 80 m height.

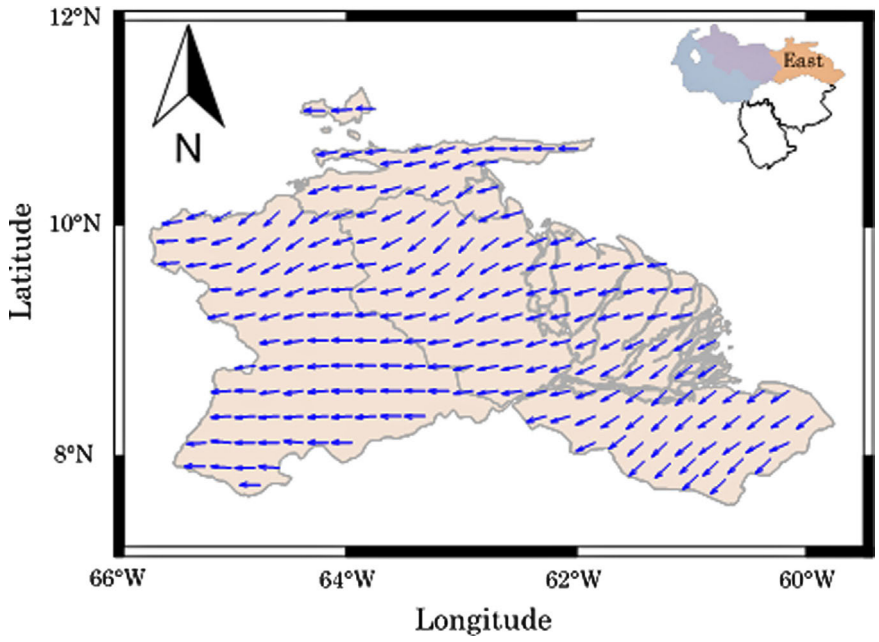

Fig. 15. Map of prevailing wind direction in East region at 80 m height.

than 600 W/m^2) and Falcón with a density power around 400–600 W/m^2. The good wind conditions in the East zone are also worthy of note, mainly in the states of Anzoátegui, Sucre, and Nueva Esparta where wind-power density values between 200 and 600 W/m^2 have been obtained. In the case of the West zone, only in the state of Zulia, and in two neighbouring areas (at the north and west of this state) values of 200–600 W/m^2 wind-power density have been found.

Results of wind density have been processed to produce a better idea of the quality of the wind conditions over the analysed surface and the exploitable areas. Table 4 shows the available surface (km^2) classified per power-density level in each of the considered zones (values in brackets refer to the percentage of surface in relation to the total surface of each zone). According to the classification of wind-power density provided in [28], 13.05% of northern Venezuela has moderate wind conditions (200–400 W/m^2), 3.07% has good conditions (400 – 600 W/m^2), and 0.91% has excellent conditions (> 600 W/m^2).

5. Conclusion

This paper presents the first wind-resource atlas of Venezuela using datasets of wind observations recorded on-site at meteorological stations between 2005 and 2007. Hourly recorded observation of wind speed and of direction of 32 anemometer masts

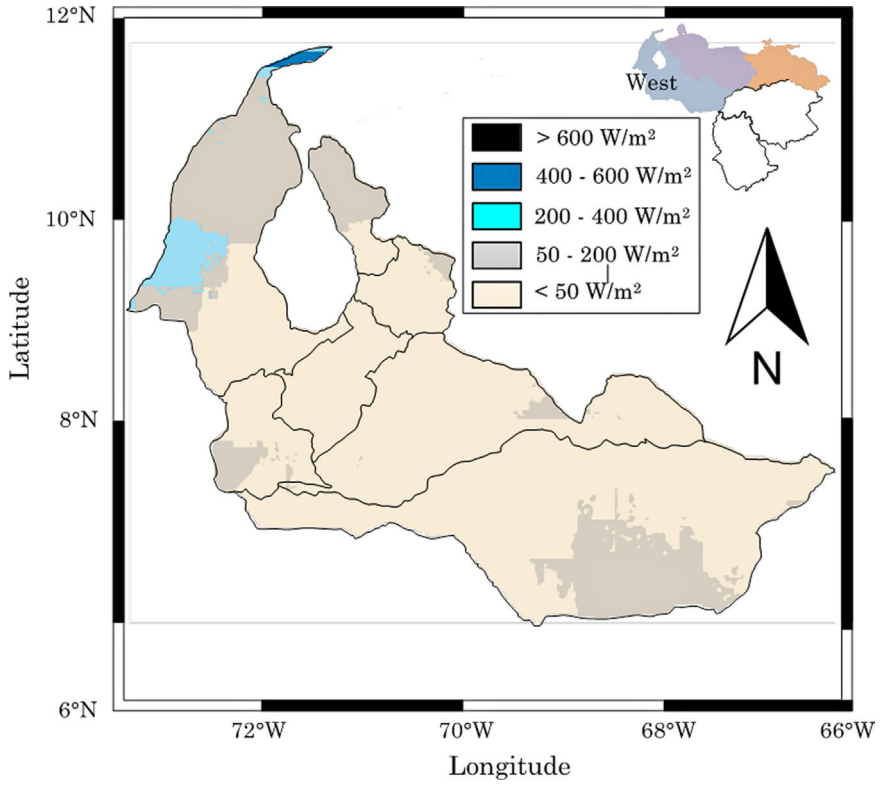

Fig. 16. Map of wind-power density in West zone at 80 m height.

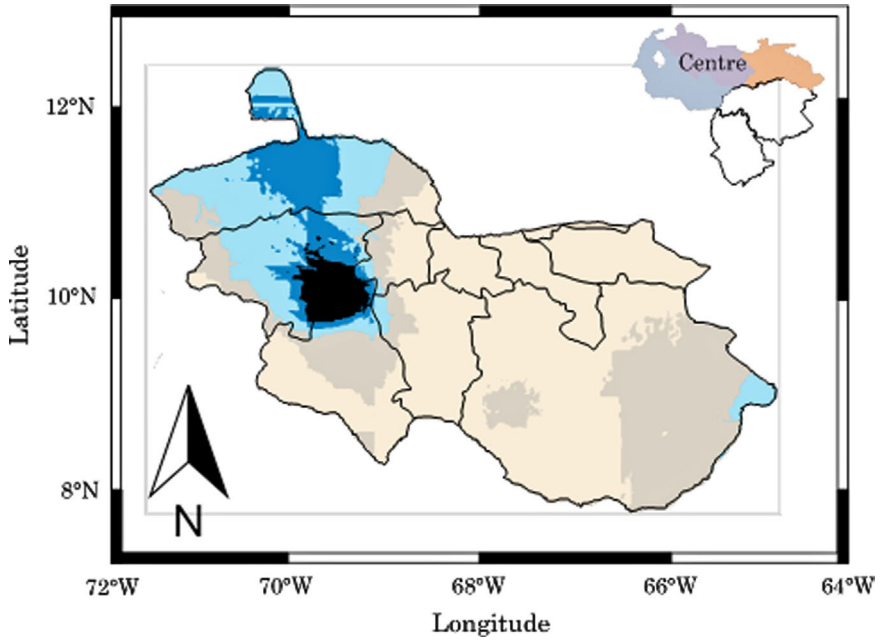

Fig. 17. Map of wind-power density in Central zone at 80 m height.

belonging to the meteorological network of the MSVAF are considered in the creation of this atlas. An implementation of *Mass-conservation Wind-Flow Model* in OpenWind software is used to calculate wind resources at each anemometer mast. This Venezuelan wind atlas has been divided into three maps representative of three regions: West, Central and East. Results are presented in the form of individual regions: traditional maps of mean wind speed for each direction and maps of wind-power density.

The results obtained in the analysis performed herein show that mean wind speed at a height of 80 m ranges between approximately 2 and 13 m/s, and that values above 6.0 m/s are found in Zulia, Falcon, Lara, Anzoátegui, Sucre, and Nueva Esparta. The direction east is the predominant wind direction in the East

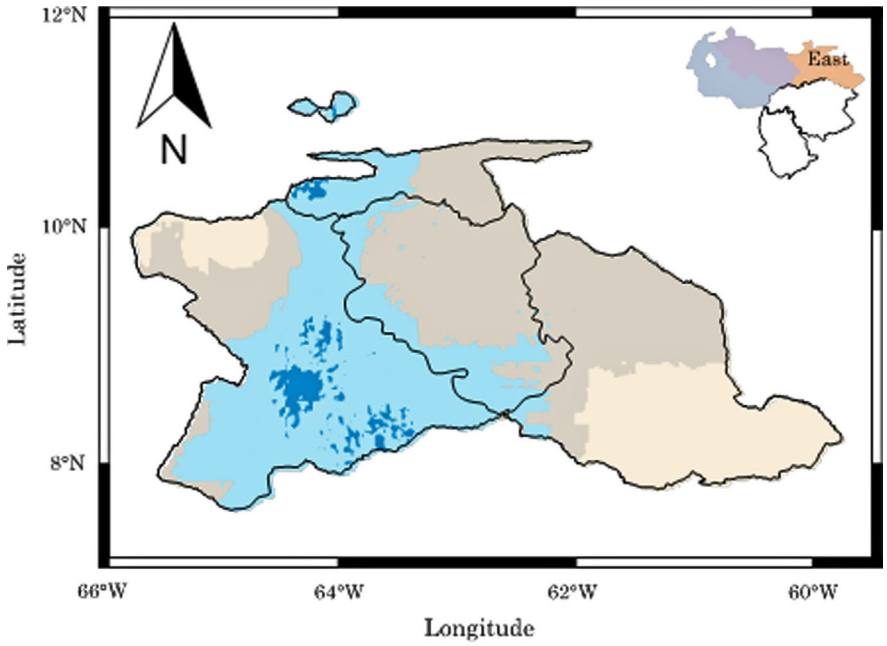

Fig. 18. Map of wind-power density in East zone at 80 m height.

Table 4
Available surface (km^2) classified per wind power density level.

Power density (W/m^2)	West zone	Central zone	East zone	Total
< 50	42,090 (22.25%)	43,729 (24.28%)	41,694 (32.53%)	127,513 (25.63%)
50–200	141,163 (74.62%)	96,152 (53.39%)	47,917 (37.39%)	285,231 (57.34%)
200–400	5305 (2.80%)	23,827 (13.23%)	35,769 (27.91%)	64,901 (13.05%)
400–600	594 (0.31%)	11,937 (6.63%)	2749 (2.15%)	15,280 (3.07%)
> 600	32 (0.02%)	4447 (2.47%)	27 (0.02%)	4506 (0.91%)

and Central regions. A surface area of 13.05% of total northern Venezuela shows moderate wind conditions (200–400 W/m^2); 3.07% (64,901 km^2) has good conditions (400–600 W/m^2); and 0.91% (15,250 km^2) has excellent conditions (> 600 W/m^2). The wind atlas created in this paper shows that suitable areas are available in the northern region to develop wind-energy projects. Wind-energy resources can be used commercially (utility-scale) in Venezuela in a large part of northern Venezuela and there are also excellent conditions for wind-power production at micro-scale application, both on- and off-grid.

References

[1] Massabie G. Venezuela: a petro-state using renewable energies: a contribution to the global debate about new renewable energies for electricity generation. 1st ed. Wiesbaden: VS Verlag für Sozialwissenschaften; 2008.
[2] Gonzalez-Longatt F. Evaluation of reactive power compensations for the phase I of Paraguaná wind based on system voltages. In: Proceedings of 39th annual conference of the IEEE industrial electronics society (IECON 2013); 2013. p. 1627–31.
[3] Gonzalez-Longatt F. Systemic impact caused by the integration of La Guajira wind farm. In: Proceedings of 39th annual conference of the IEEE industrial electronics society (IECON 2013); 2013. p. 1893–7.
[4] González-Longatt F, Méndez J, Villasana R. Preliminary evaluation of wind energy utilization on Margarita Island, Venezuela. In: Proceedings of the sixth international worshop on large-scale of integration of wind power and transmission networks for offshore wind farms, Delft, Netherlands; 2006.p. 26–8.
[5] González-Longatt F, Méndez J, Villasana R, Peraza C. Wind energy resource evaluation on Venezuela: Part I. In: Proceedings of the Nordic wind power conference (NWPC); 2006. p. 1–5.
[6] Alamdari P, Nematollahi O, Mirhosseini M. Assessment of wind energy in Iran: a review. Renew Sustain Energy Rev 2012;16:836–60.
[7] İlkiliç C. Wind energy and assessment of wind energy potential in Turkey. Renew Sustain Energy Rev 2012;16:1165–73.
[8] Đurišić Ž, Mikulović J. Assessment of the wind energy resource in the South Banat region, Serbia. Renew Sustain Energy Rev 2012;15:3014–23.
[9] Ahmed AS. Renew Sustain Energy Rev 2012;16:1528–36.
[10] Jervase JA, Al-Lawati AM. Wind energy potential assessment for the Sultanate of Oman. Renew Sustain Energy Rev 2012;16:1496–7.
[11] Chadee XT, Clarke RM. Large-scale wind energy potential of the Caribbean region using near-surface reanalysis data. Renew Sustain Energy Rev 2014;30:45–58.
[12] Contreras VM, Elistratov VV. Evaluación técnica del recurso eólico en Venezuela; 2013.
[13] LnEG. Avaliação do recurso solar e eólico para a Venezuela. Available from: ⟨http://www.lneg.pt/iedt/projectos/451/⟩; 2014 [accessed 21.02.14]].
[14] Bailey BH, Beaucage P, Bernadett DW, Brower M. Wind resource assessment: a practical guide to developing a wind project. UK: John Wiley & Sons; 2012.
[15] Serrano González J, Burgos Payán M, Riquelme Santos JM, González-Longatt F. A review and recent developments in the optimal wind-turbine micro-siting problem. Renew Sustain Energy Rev 2014;30:133–44.
[16] Strack M, Riedel V. State of the art in application of flow models for micrositing. In: Proceedings of the German wind energy conference (DEWEK); 2004.
[17] Phillips GT. Preliminary user's guide for the NOABL objective analysis code. (Special report, 15 June 1977–15 June 1978). 1979.
[18] Geai P. Methode d'Interpolation et de reconstitution tridi-mensionnelle d'un champ de vent: le code d'analyse objective MINERVE. (EDF R&D report HE/34-87.03). 1987.
[19] Brower M. Validation of the WindMap program and development of Meso-Map. In: Proceedings of the AWEA's windpower conference. Washington, DC; 1979.
[20] AWS Truepower. "OpenWind," 7.00 ed. Available from: ⟨http://www.awsopenwind.org⟩; 2013 [accessed 19.12.13].
[21] Hartkamp AD, Beurs KD, Stein A, White JW. Interpolation techniques for climate variables. 1999.
[22] Goodin WR, McRa GJ, Seinfeld JH. A comparison of interpolation methods for sparse data: application to wind and concentration fields. J Appl Meteorol 1979;18:761.

[23] Weibull W. A statistical distribution function of wide applicability. J Appl Mech 1951;18:293–7.
[24] Loureiro JB, Soares DV, Rodrigues, José Luiz Fontoura A, Pinho FT, Freire APS. Investigation of turbulent flow over a steep hill using laser doppler anemometry. 2005.
[25] NASA. Aerodynamic roughness – vegetation aerodynamic roughness parameters in the Amazon Basin. Available from: ⟨http://www-radar.jpl.nasa.gov/carbon/ab/ar.htm⟩; 2013 [accessed 04.06.13].
[26] Saatchi S, Rodriguez E, Denning S, Dubayah R. Estimation of aerodynamic roughness from synergistic use of satellite imagery. In: Proceedings of the international geoscience and remote sensing symposium (IGARSS). Sydney, Australia; 2001.
[27] LBA-ECO LC-15 Aerodynamic roughness maps of vegetation canopies, Amazon Basin; 2000.
[28] Al-Nassar W, Alhajraf S, Al-Enizi A, Al-Awadhi L. Potential wind power generation in the State of Kuwait. Renew Energy 2005;30:2149–61.